



HHS Public Access

Author manuscript

Bioorg Med Chem Lett. Author manuscript; available in PMC 2017 October 01.

Published in final edited form as:

Bioorg Med Chem Lett. 2016 October 1; 26(19): 4724–4728. doi:10.1016/j.bmcl.2016.08.042.

Imaging human melanoma using a novel Tc-99m-labeled lactam bridge-cyclized alpha-MSH peptide

Liqin Liu^a, Jingli Xu^b, Jianquan Yang^b, Changjian Feng^c, and Yubin Miao^{b,*}

^aSchool of Chemistry and Biological Engineering, University of Science and Technology Beijing, Beijing 100083, P. R. China

^bDepartment of Radiology, University of Colorado Denver, Aurora, CO 80045, USA

^cCollege of Pharmacy, University of New Mexico, Albuquerque, NM 87131, USA

Abstract

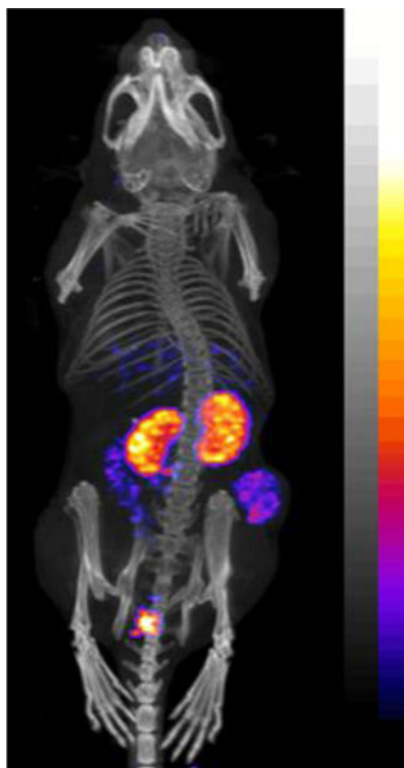
In this study, the human melanoma targeting property of ^{99m}Tc(EDDA)-HYNIC-AocNle-CycMSH_{hex} {hydrazinonicotinamide-8-aminooctanoic acid-Nle-c[Asp-His-DPhe-Arg-Trp-Lys]-CONH₂} was determined in M21 human melanoma-xenografts to demonstrate its potential for human melanoma imaging. The IC₅₀ value of HYNIC-AocNle-CycMSH_{hex} was 0.48 ± 0.01 nM in M21 human melanoma cells (1,281 receptors/cell). The M21 human melanoma uptake of ^{99m}Tc(EDDA)-HYNIC-AocNle-CycMSH_{hex} was 4.03 ± 1.25, 3.26 ± 1.23 and 3.36 ± 1.48% ID/g at 0.5, 2 and 4 h post-injection, respectively. Approximately 92% of injected dose cleared out the body via urinary system at 2 h post-injection. ^{99m}Tc(EDDA)-HYNIC-AocNle-CycMSH_{hex} showed high tumor/blood, tumor/muscle and tumor/skin uptake ratios after 2 h post-injection. The M21 human melanoma-xenografted tumor lesions were clearly visualized by SPECT/CT using ^{99m}Tc(EDDA)-HYNIC-AocNle-CycMSH_{hex} as an imaging probe at 2 h post-injection. Overall, ^{99m}Tc(EDDA)-HYNIC-AocNle-CycMSH_{hex} exhibited favorable human melanoma imaging property, highlighting its potential as an imaging probe for human metastatic melanoma detection.

Graphical abstract

SPECT/CT image of a M21 human melanoma-xenografted nude mouse using ^{99m}Tc(EDDA)-HYNIC-AocNle-CycMSH_{hex} as an imaging probe.

Corresponding Author: Yubin Miao, 12700 East 19th Ave., MS C278, Department of Radiology, School of Medicine, University of Colorado Denver, Aurora, CO 80045, USA. Phone: (303) 724-3763; yubin.miao@ucdenver.edu.

Publisher's Disclaimer: This is a PDF file of an unedited manuscript that has been accepted for publication. As a service to our customers we are providing this early version of the manuscript. The manuscript will undergo copyediting, typesetting, and review of the resulting proof before it is published in its final citable form. Please note that during the production process errors may be discovered which could affect the content, and all legal disclaimers that apply to the journal pertain.



Keywords

Alpha-melanocyte stimulating hormone; ^{99m}Tc -labeled lactam bridge-cyclized peptide; human melanoma targeting; SPECT/CT

Malignant melanoma is the most lethal form of skin cancer. Despite that melanoma is less than 5% of skin cancer cases, it accounting for 75% of deaths of skin cancer.¹ Metastatic melanoma is extremely aggressive and leads to high mortality of melanoma. Thus, it is desirable to develop receptor-targeting peptide radiopharmaceuticals for melanoma imaging and therapy. Melanocortin-1 (MC1) receptor is a distinct molecular target due to its over-expression on murine and human melanoma cells.²⁻⁶ Over the past several years, we and others have developed ^{99m}Tc -labeled α -MSH peptides⁷⁻¹⁴ to target the MC1 receptors for melanoma imaging, taking advantage of the ideal imaging properties of ^{99m}Tc (140-keV γ -photon and 6 h half-life) and its wide application in nuclear medicine. Specifically, we have developed a novel class of ^{99m}Tc -labeled lactam bridge-cyclized α -MSH peptides building upon the construct of GGNle-CycMSH_{hex} {Gly-Gly-Nle-c[Asp-His-DPhe-Arg-Trp-Lys]-CONH₂}¹⁰. We conjugated bifunctional metal chelators such as mercaptoacetyltriglycine (MAG₃), Ac-Cys-Gly-Gly-Gly (AcCG₃) and hydrazinonicotinamide (HYNIC) to GGNle-CycMSH_{hex} to examine which metal chelator was suitable for ^{99m}Tc in terms of melanoma targeting and clearance properties. Interestingly, ^{99m}Tc (EDDA)-HYNIC-GGNle-CycMSH_{hex} exhibited higher melanoma uptake and faster urinary clearance than ^{99m}Tc -MAG₃-GGNle-CycMSH_{hex} and ^{99m}Tc -AcCG₃-GGNle-CycMSH_{hex} in B16/F1 melanoma-bearing C57 mice.¹⁰

Recently, building upon the success of $^{99m}\text{Tc}(\text{EDDA})\text{-HYNIC-GGNle-CycMSH}_{\text{hex}}$, we further examined the effects of amino acid, hydrocarbon and PEG linkers on the melanoma targeting and clearance properties of ^{99m}Tc -labeled $\text{CycMSH}_{\text{hex}}$ peptides.¹⁴ Specifically, we inserted -GlyGlyGly- (GGG), -GlySerGly- (GSG), -Aoc- (8-aminooctanoic acid) and -PEG₂-linkers between the HYNIC and Nle-CycMSH_{hex} moiety to generate new HYNIC-linker-Nle-CycMSH_{hex} peptides. The introduction of -GGG-, -GSG-, -Aoc- and -PEG₂-linkers retained low nanomolar (0.3–0.8 nM) MC1 receptor binding affinities of the peptides. Interestingly, we found that the introduction of the Aoc linker enhanced the uptake of $^{99m}\text{Tc}(\text{EDDA})\text{-HYNIC-AocNle-CycMSH}_{\text{hex}}$ in B16/F1 melanoma. $^{99m}\text{Tc}(\text{EDDA})\text{-HYNIC-AocNle-CycMSH}_{\text{hex}}$ displayed high melanoma uptake ($22.8 \pm 1.71\%$ ID/g at 2 h post-injection) and high tumor to normal organ uptake ratios.¹⁴ The B16/F1 melanoma lesions were clearly visualized by single photon emission computed tomography (SPECT)/CT using $^{99m}\text{Tc}(\text{EDDA})\text{-HYNIC-AocNle-CycMSH}_{\text{hex}}$ as an imaging probe at 2 h post-injection.¹⁴

It was reported that the MC1 receptors are expressed on more than 80% of human metastatic melanoma samples.¹⁵ Meanwhile, a bank of human melanoma cell lines that are derived from primary and metastatic melanoma lesions (melanonic or amelanonic) displayed MC1 receptors. The receptor densities range from 900 to 5700 receptors per cell.⁴ In our previous work, we examined the MC1 receptor density of M21 human melanoma cells by saturation binding assay. The MC1 receptor density of the M21 cells was 1,281 receptors per cell.¹⁶ In this study, we managed to examine whether we could visualize the M21 human melanoma xenografts by SPECT/CT using $^{99m}\text{Tc}(\text{EDDA})\text{-HYNIC-AocNle-CycMSH}_{\text{hex}}$ as an imaging probe. Successful imaging of the M21 human melanoma xenografts with low MC1 receptor densities will demonstrate its potential for human melanoma imaging. Thus, we prepared $^{99m}\text{Tc}(\text{EDDA})\text{-HYNIC-AocNle-CycMSH}_{\text{hex}}$ and examined its receptor binding affinity, cellular internalization and efflux properties in M21 human melanoma cells, and determined its melanoma targeting and imaging properties in M21 human melanoma-xenografted nude mice in this study.

Firstly, HYNIC-AocNle-CycMSH_{hex} (Figure 1) was synthesized and purified by reverse phase high pressure liquid chromatography (RP-HPLC) according to our published procedure.¹⁴ After the HPLC purification, HYNIC-AocNle-CycMSH_{hex} displayed greater than 90% purity. The identity of HYNIC-AocNle-CycMSH_{hex} was confirmed by electrospray ionization mass spectrometry. The IC₅₀ value of HYNIC-AocNle-CycMSH_{hex}, and HYNIC-PEG₂Nle-CycMSH_{hex} was 0.48 ± 0.01 nM in M21 human melanoma cells (Figure 1). $^{99m}\text{Tc}(\text{EDDA})\text{-HYNIC-AocNle-CycMSH}_{\text{hex}}$ was readily prepared according to our published procedure¹⁴ with greater than 95% radiolabeling yield, and was completely separated from its excess non-labeled peptide by RP-HPLC. The retention time of $^{99m}\text{Tc}(\text{EDDA})\text{-HYNIC-AocNle-CycMSH}_{\text{hex}}$ was 24 min. $^{99m}\text{Tc}(\text{EDDA})\text{-HYNIC-AocNle-CycMSH}_{\text{hex}}$ was stable in mouse serum at 37 °C for 4 h. Cellular internalization and efflux properties of $^{99m}\text{Tc}(\text{EDDA})\text{-HYNIC-AocNle-CycMSH}_{\text{hex}}$ were examined in M21 human melanoma cells. Figure 2 illustrates the internalization and efflux of $^{99m}\text{Tc}(\text{EDDA})\text{-HYNIC-AocNle-CycMSH}_{\text{hex}}$. $^{99m}\text{Tc}(\text{EDDA})\text{-HYNIC-AocNle-CycMSH}_{\text{hex}}$ exhibited rapid cellular internalization and prolonged cellular retention. Approximately 66% and 82% of $^{99m}\text{Tc}(\text{EDDA})\text{-HYNIC-AocNle-CycMSH}_{\text{hex}}$ was internalized in the cells after 20 and

120 min of incubation. Cellular efflux results indicated that 66% of the $^{99m}\text{Tc}(\text{EDDA})\text{-HYNIC-AocNle-CycMSH}_{\text{hex}}$ activity remained inside the cells at 2 h of incubation in the culture medium (Figure 2).

Secondly, the melanoma targeting and pharmacokinetic properties of $^{99m}\text{Tc}(\text{EDDA})\text{-HYNIC-AocNle-CycMSH}_{\text{hex}}$ were determined in M21 human melanoma-xenografted nude mice. The biodistribution results of $^{99m}\text{Tc}(\text{EDDA})\text{-HYNIC-AocNle-CycMSH}_{\text{hex}}$ are presented in Table 1. $^{99m}\text{Tc}(\text{EDDA})\text{-HYNIC-AocNle-CycMSH}_{\text{hex}}$ displayed rapid melanoma uptake. The tumor uptake was 4.03 ± 1.25 and $3.26 \pm 1.23\%$ ID/g at 0.5 and 2 h post-injection, respectively. $^{99m}\text{Tc}(\text{EDDA})\text{-HYNIC-AocNle-CycMSH}_{\text{hex}}$ exhibited prolonged tumor retention, with 3.36 ± 1.48 and $1.32 \pm 0.34\%$ ID/g of tumor uptake at 4 and 24 h post-injection. The co-injection of non-radioactive NDP-MSH blocked 80% of the tumor uptake at 2 h post-injection, demonstrating that the tumor uptake was MC1 receptor-mediated. Whole-body clearance of $^{99m}\text{Tc}(\text{EDDA})\text{-HYNIC-AocNle-CycMSH}_{\text{hex}}$ was rapid, with approximately 91% of the injected dose being washed out of the body via urinary system by 2 h post-injection. Ninety-six percent of the injected dose cleared out of the body by 24 h post-injection. Kidneys are the normal organs with the highest uptake of $^{99m}\text{Tc}(\text{EDDA})\text{-HYNIC-AocNle-CycMSH}_{\text{hex}}$. The renal uptake was 10.19 ± 1.14 , 4.62 ± 1.27 , and $3.55 \pm 1.33\%$ ID/g at 0.5, 2 and 4 h post-injection, respectively. At 24 h post-injection, the kidney uptake was $1.17 \pm 0.37\%$ ID/g. The co-injection of NDP-MSH didn't reduce the renal uptake, indicating that the renal uptake of $^{99m}\text{Tc}(\text{EDDA})\text{-HYNIC-AocNle-CycMSH}_{\text{hex}}$ was not receptor-mediated. The accumulation of $^{99m}\text{Tc}(\text{EDDA})\text{-HYNIC-AocNle-CycMSH}_{\text{hex}}$ in other normal organs was much lower than kidneys. High tumor/blood and tumor/normal organ uptake ratios were demonstrated as early as 2 h post-injection. The representative whole-body SPECT/CT image is presented in Figure 3. The M21 human melanoma xenografts were clearly visualized by SPECT/CT using $^{99m}\text{Tc}(\text{EDDA})\text{-HYNIC-AocNle-CycMSH}_{\text{hex}}$ as an imaging probe at 2 h post-injection.

Both receptor binding affinity and specific activity are important factors to take into account in developing receptor-targeting imaging agents when the receptor density is relatively low. It was reported that $^{188}\text{Re-CCMSH}$ and $^{188}\text{Re-(Arg}^{11}\text{)CCMSH}$ displayed fast tumor uptake in TXM13 human melanoma xenografts.⁴ For instance, the TXM13 tumor uptake was 1.98 ± 0.26 for $^{188}\text{Re-CCMSH}$ and $3.06 \pm 0.68\%$ ID/g for $^{188}\text{Re-(Arg}^{11}\text{)CCMSH}$ at 1 h post-injection.⁴ At 4 h post-injection, the tumor uptake was 2.20 ± 0.24 for $^{188}\text{Re-CCMSH}$ and $2.02 \pm 0.27\%$ ID/g for $^{188}\text{Re-(Arg}^{11}\text{)CCMSH}$. However, the renal uptake of $^{188}\text{Re-(Arg}^{11}\text{)CCMSH}$ was only 50% of that of $^{188}\text{Re-CCMSH}$.⁴ It is worthwhile to note that the receptor density of TXM13 cells is higher than that of M21 human melanoma cells (5,500 vs. 1,281 receptor/cell). As shown in table 1, the M21 tumor uptake was 4.03 ± 1.25 and $3.36 \pm 1.48\%$ ID/g at 0.5 and 4 h post-injection for $^{99m}\text{Tc}(\text{EDDA})\text{-HYNIC-AocNle-CycMSH}_{\text{hex}}$. The slightly higher tumor uptake of $^{99m}\text{Tc}(\text{EDDA})\text{-HYNIC-AocNle-CycMSH}_{\text{hex}}$ is likely due to its sub-nanomolar MC1 receptor binding affinity. Besides strong receptor binding affinity, high specific activity is another key factor which contributes to successful receptor-targeting imaging when the receptor density is relatively low. As shown in Figure 1, 10 nM of HYNIC-AocNle-CycMSH_{hex} could completely block the MC1 receptor binding. Thus, it is important to achieve high specific activity during radiolabeling

and purification processes. Both $^{188}\text{Re}-(\text{Arg}^{11})\text{CCMSH}$ and $^{99\text{m}}\text{Tc}(\text{EDDA})\text{-HYNIC-AocNle-CycMSH}_{\text{hex}}$ were purified by HPLC to reach the maximum specific activity by getting rid of any unlabeled cold peptide.

The experimental details are presented in References and notes.^{17–20}

In conclusion, the human melanoma targeting and imaging properties of $^{99\text{m}}\text{Tc}(\text{EDDA})\text{-HYNIC-AocNle-CycMSH}_{\text{hex}}$ were determined in M21 human melanoma-xenografted nude mice in this study. Overall, the properties of rapid melanoma uptake and fast urinary clearance of $^{99\text{m}}\text{Tc}(\text{EDDA})\text{-HYNIC-AocNle-CycMSH}_{\text{hex}}$ underscored its potential as an imaging agent for metastatic human melanoma detection in the future.

Acknowledgments

We thank Dr. Fabio Gallazzi for his technical assistance. This work was partially supported by University of Colorado Denver start-up fund and the NIH grant R15CA173516.

REFERENCES AND NOTES

1. Siegel RL, Kimberly DM, Jemal A. Cancer Statistics, 2016. *CA Cancer J Clin.* 2016; 66:7. [PubMed: 26742998]
2. Siegrist W, Solca F, Stutz S, Giuffre L, Carrel S, Girard J, Eberle AN. *Cancer Res.* 1989; 49:6352. [PubMed: 2804981]
3. Tatro JB, Reichlin S. *Endocrinology.* 1987; 121:1900. [PubMed: 2822378]
4. Miao Y, Whitener D, Feng W, Owen NK, Chen J, Quinn TP. *Bioconjug Chem.* 2003; 14:1177. [PubMed: 14624632]
5. Miao Y, Owen NK, Whitener D, Gallazzi F, Hoffman TJ, Quinn TP. *Int J Cancer.* 2002; 101:480. [PubMed: 12216078]
6. Chen J, Cheng Z, Hoffman TJ, Jurisson SS, Quinn TP. *Cancer Res.* 2000; 60:5649. [PubMed: 11059756]
7. Raposinho PD, Correia JD, Alves S, Botelho MF, Santos AC, Santos I. *Nucl Med Biol.* 2008; 35:91. [PubMed: 18158948]
8. Raposinho PD, Xavier C, Correia JD, Falcao S, Gomes P, Santos I. *J Biol Inorg Chem.* 2008; 13:449. [PubMed: 18183429]
9. Morais M, Oliveira BL, Correia JD, Oliveira MC, Jiménez MA, Santos I, Raposinho PD. *J Med Chem.* 2013; 56:1961. [PubMed: 23414214]
10. Guo H, Gallazzi F, Miao Y. *Mol Pharmaceutics.* 2013; 10:1400.
11. Miao Y, Benwell K, Quinn TP. *J Nucl Med.* 2007; 48:73. [PubMed: 17204701]
12. Kasten BB, Ma X, Liu H, Hayes TR, Barnes CL, Qi S, Cheng K, Bortorff SC, Slocumb WS, Wang J, Cheng Z, Benny PD. *Bioconjug Chem.* 2014; 25:579. [PubMed: 24568284]
13. Jiang H, Kasten BB, Liu H, Qi S, Liu Y, Tian M, Barnes CL, Zhang H, Cheng Z, Benny PD. *Bioconjug Chem.* 2012; 23:2300. [PubMed: 23110503]
14. Guo H, Miao Y. *J Nucl Med.* 2014; 55:2057. [PubMed: 25453052]
15. Tatro JB, Wen Z, Entwistle ML, Atkins MB, Smith TJ, Reichlin S, Murphy JR. *Cancer Res.* 1992; 52:2545. [PubMed: 1314697]
16. Yang J, Guo H, Miao Y. *Nucl Med Biol.* 2010; 37:873. [PubMed: 21055617]
17. In vitro competitive binding assay: Amino acid and resin were purchased from Advanced ChemTech Inc (Louisville, KY) and Novabiochem (San Diego, CA) for peptide synthesis All other chemicals used in this study were purchased from Thermo Fischer Scientific (Waltham, MA) and used without further purification HYNIC-AocNle-CycMSH_{hex} was synthesized using fluorenylmethyloxy carbonyl (Fmoc) chemistry, purified by reverse phase-high performance liquid chromatography (RP-HPLC) and characterized by liquid chromatography-mass spectrometry (LC-

MS) according to our published procedure¹⁴ Generally, 70 μmol of resin, 210 μmol of each Fmoc-protected amino acid and 210 μmol of Boc-HYNIC were used for the synthesis. M21 human melanoma cells were supplied by Dr David A Cheresch from the Department of Pathology, Moores University of California-San Diego Cancer Center. ^{125}I -Tyr²-[Nle⁴, D-Phe⁷]- α -MSH (^{125}I -Tyr²)-NDP-MSH) was obtained from PerkinElmer, Inc. (Waltham, MA) for receptor binding assay. The MC1 receptor binding affinity of HYNIC-AocNle-CycMSH_{hex} was determined in M21 human melanoma cells by *in vitro* competitive receptor binding assay. The receptor binding assay was replicated in triplicate. The M21 cells (1.5×10^5 cells/well, n=3) were incubated at 37 °C for 2 h with approximately 30,000 counts per minute (cpm) of ^{125}I -Tyr²)-NDP-MSH in the presence of 10^{-12} to 10^{-5} M of the peptide in 0.3 mL of binding medium {Modified Eagle's medium with 25 mM N-(2-hydroxyethyl)-piperazine-N'-(2-ethanesulfonic acid), pH 7.4, 0.2% bovine serum albumin (BSA), 0.3 mM 1,10-phenathroline}. The binding medium was aspirated after the incubation. The cells were rinsed twice with 0.5 ml of ice-cold pH 7.4, 0.2% BSA/0.01 M phosphate buffered saline (PBS) and lysed in 0.5 mL of 1 N NaOH for 5 min. The cells were harvested and measured in a Wallac 1480 automated gamma counter (PerkinElmer, NJ). The IC₅₀ value was calculated using the Prism software (GraphPad Software, La Jolla, CA, USA).

18. Internalization and efflux: $^{99\text{m}}\text{Tc}$ was purchased from Cardinal Health (Denver, CO) for peptide radiolabeling. $^{99\text{m}}\text{Tc}$ (EDDA)-HYNIC-AocNle-CycMSH_{hex} was prepared according to our published procedure.¹⁴ Cellular internalization and efflux of $^{99\text{m}}\text{Tc}$ (EDDA)-HYNIC-AocNle-CycMSH_{hex} were evaluated in M21 melanoma cells. After being washed twice with binding medium [modified Eagle's medium with 25 mM N-(2-hydroxyethyl)-piperazine-N'-(2-ethanesulfonic acid), pH 7.4, 0.2% bovine serum albumin (BSA), 0.3 mM 1,10-phenathroline], the M21 cells seeded in cell culture plates were incubated at 37°C for 20, 40, 60, 90 and 120 min (n=3) in the presence of approximate 200,000 counts per minute (cpm) of HPLC-purified $^{99\text{m}}\text{Tc}$ (EDDA)-HYNIC-AocNle-CycMSH_{hex}. After incubation, the reaction medium was aspirated and the cells were rinsed with 2×0.5 mL of ice-cold pH 7.4, 0.2% BSA / 0.01 M PBS. Cellular internalization of $^{99\text{m}}\text{Tc}$ (EDDA)-HYNIC-AocNle-CycMSH_{hex} was assessed by washing the cells with acidic buffer [40 mM sodium acetate (pH 4.5) containing 0.9% NaCl and 0.2% BSA] to remove the membrane-bound radioactivity. The remaining internalized radioactivity was obtained by lysing the cells with 0.5 mL of 1 N NaOH for 5 min. Membrane-bound and internalized $^{99\text{m}}\text{Tc}$ (EDDA)-HYNIC-AocNle-CycMSH_{hex} activity was counted in a gamma counter. Cellular efflux of $^{99\text{m}}\text{Tc}$ (EDDA)-HYNIC-AocNle-CycMSH_{hex} was determined by incubating the M21 cells with $^{99\text{m}}\text{Tc}$ (EDDA)-HYNIC-AocNle-CycMSH_{hex} for 2 h at 37 °C, removing non-specific-bound activity with 2 × 0.5 mL of ice-cold PBS rinse, and monitoring radioactivity released into cell culture medium. At time points of 20, 40, 60, 90 and 120 min, the radioactivity on the cell surface and inside the cells were separately collected and counted in a gamma counter.
19. Biodistribution studies: All animal studies were conducted in compliance with Institutional Animal Care and Use Committee approval. The nude mice were subcutaneously inoculated with 5×10^6 M21 cells on the right flank for each mouse to generate melanoma tumors. The weights of tumors reached approximately 0.1–0.2 g 21 days post cell inoculation. Each melanoma-xenografted nude mouse was injected with 0.037 MBq of $^{99\text{m}}\text{Tc}$ (EDDA)-HYNIC-AocNle-CycMSH_{hex} via the tail vein. Groups of 5 mice were sacrificed at 0.5, 2, 4 and 24 h post-injection, tumor and organs of interest were harvested, weighed and counted in a Wallace 1480 automated gamma counter (PerkinElmer). Meanwhile, intestines and urine were collected and counted to evaluate the clearance of $^{99\text{m}}\text{Tc}$ (EDDA)-HYNIC-AocNle-CycMSH_{hex}. Blood was taken as 6.5% of the body weight. The tumor uptake specificity of $^{99\text{m}}\text{Tc}$ (EDDA)-HYNIC-AocNle-CycMSH_{hex} was determined by co-injecting 10 μg (6.07 nmol) of unlabeled NDP-MSH peptide at 2 h post-injection. The mice were sacrificed at 2 h post-injection and the tumors and organs of interest were harvested, weighed and counted. Statistical analysis was performed using the Student's t-test for unpaired data. A 95% confidence level was chosen to determine the significance of difference in tumor and renal uptake of $^{99\text{m}}\text{Tc}$ (EDDA)-HYNIC-AocNle-CycMSH_{hex} with/without NDP-MSH co-injection. The differences at the 95% confidence level ($p < 0.05$) were considered significant.
20. Human melanoma imaging: Approximately 7.4 MBq of $^{99\text{m}}\text{Tc}$ (EDDA)-HYNIC-AocNle-CycMSH_{hex} was injected in a M21 human melanoma-xenografted nude mouse via the tail vein for melanoma imaging. The mouse was euthanized at 2 h post-injection for small animal SPECT/CT (nanoScan SPECT/CT, Mediso) imaging. The CT scan was immediately followed by the whole-

body SPECT scan. Reconstructed SPECT and CT data were visualized and co-registered using VivoQuant (inviCRO, Boston, MA).

Author Manuscript

Author Manuscript

Author Manuscript

Author Manuscript

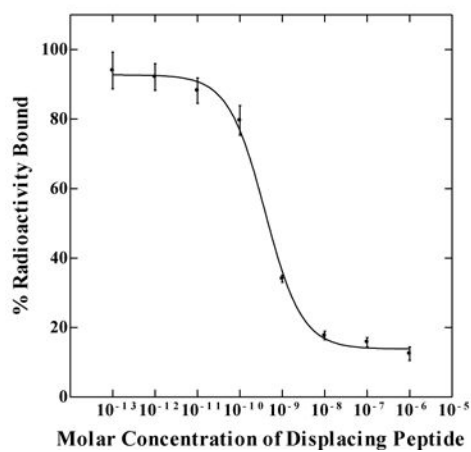
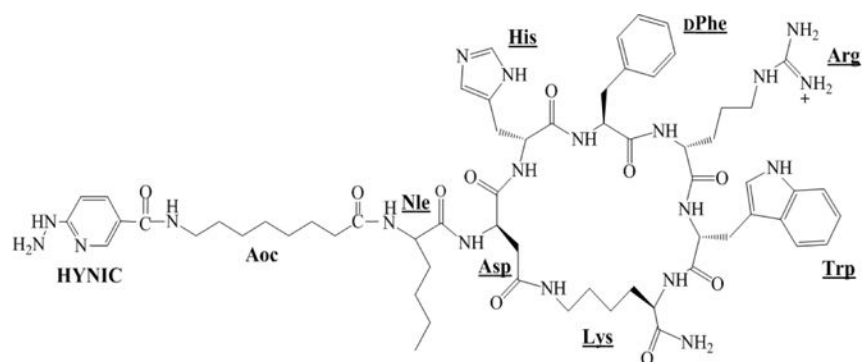


Figure 1. Schematic structure and *in vitro* competitive binding curve of HYNIC-AocNle-CycMSH_{hex}. The IC_{50} value of HYNIC-AocNle-CycMSH_{hex} was 0.48 ± 0.01 nM in M21 human melanoma cells.

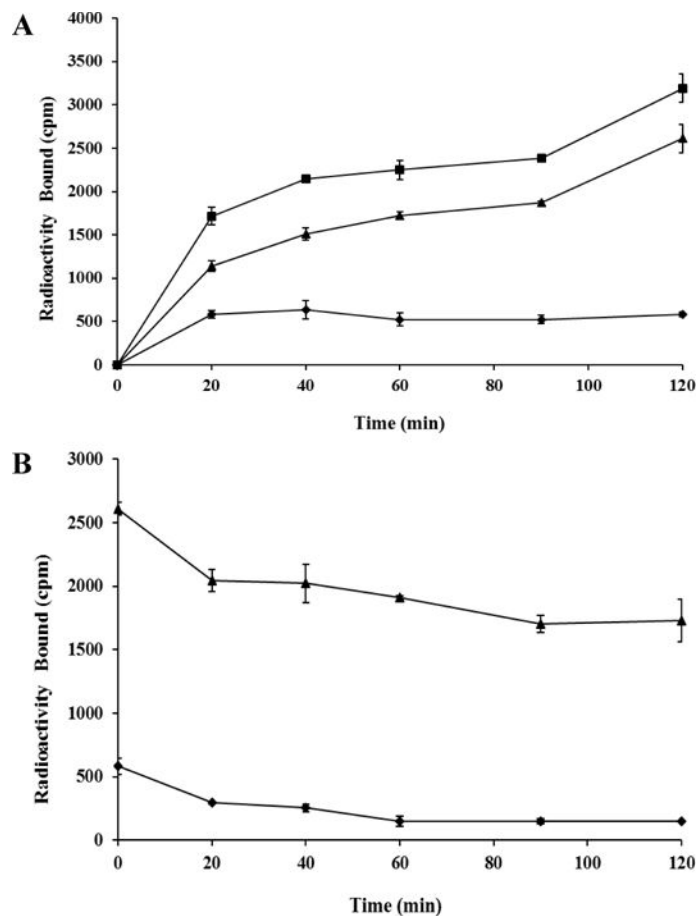


Figure 2. Cellular internalization (A) and efflux (B) of $^{99m}\text{Tc}(\text{EDDA})\text{-HYNIC-AocNle-CycMSH}_{\text{hex}}$ in M21 human melanoma cells. Total bound radioactivity (■), internalized radioactivity (▲) and cell membrane radioactivity (◆) were presented as counts per minute (cpm).

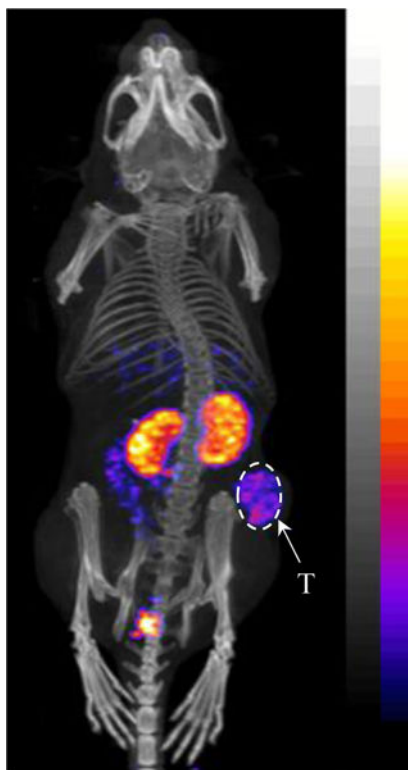


Figure 3. Representative whole-body SPECT/CT image of $^{99m}\text{Tc}(\text{EDDA})\text{-HYNIC-AocNle-CycMSH}_{\text{hex}}$ in a M21 human melanoma-xenografted nude mouse at 2 h post-injection.

Biodistribution of $^{99m}\text{Tc}(\text{EDDA})\text{-HYNIC-AocNle-CycMSH}_{\text{Hex}}$ in M21 human melanoma-xenografted nude mice. The data were presented as percent injected dose/gram or as percent injected dose (Mean \pm SD, n=5)

Table 1

Tissues	0.5 h	2 h	4 h	24 h	2 h NDP blockade
	Percent injected dose/gram (%ID/g)				
Tumor	4.03 \pm 1.25	3.26 \pm 1.23	3.36 \pm 1.48	1.32 \pm 0.34	0.66 \pm 0.12*
Brain	0.19 \pm 0.06	0.03 \pm 0.01	0.02 \pm 0.01	0.03 \pm 0.02	0.05 \pm 0.01
Blood	3.41 \pm 0.77	0.52 \pm 0.19	0.42 \pm 0.13	0.55 \pm 0.42	0.66 \pm 0.09
Heart	1.49 \pm 0.37	0.25 \pm 0.11	0.22 \pm 0.09	0.14 \pm 0.01	0.29 \pm 0.06
Lung	3.10 \pm 0.54	0.65 \pm 0.15	0.62 \pm 0.32	0.28 \pm 0.04	0.79 \pm 0.14
Liver	2.79 \pm 0.52	1.41 \pm 0.20	1.41 \pm 0.43	0.70 \pm 0.18	1.34 \pm 0.16
Spleen	1.09 \pm 0.18	0.34 \pm 0.13	0.43 \pm 0.40	0.32 \pm 0.12	0.37 \pm 0.09
Stomach	1.72 \pm 0.19	1.25 \pm 0.38	1.40 \pm 0.36	0.47 \pm 0.28	0.76 \pm 0.43
Kidneys	10.19 \pm 1.14	4.62 \pm 1.27	3.55 \pm 1.33	1.17 \pm 0.37	3.92 \pm 0.91
Muscle	0.38 \pm 0.21	0.05 \pm 0.01	0.11 \pm 0.13	0.12 \pm 0.05	0.09 \pm 0.10
Pancreas	0.57 \pm 0.22	0.23 \pm 0.06	0.17 \pm 0.04	0.18 \pm 0.07	0.27 \pm 0.10
Bone	1.10 \pm 0.24	0.26 \pm 0.15	0.30 \pm 0.14	0.23 \pm 0.09	0.11 \pm 0.11
Skin	3.99 \pm 0.90	0.59 \pm 0.10	0.68 \pm 0.33	0.47 \pm 0.16	0.55 \pm 0.07
	Percent injected dose (%ID)				
Intestines	1.92 \pm 0.29	1.87 \pm 0.72	1.98 \pm 0.51	0.72 \pm 0.08	1.65 \pm 0.73
Urine	72.03 \pm 3.52	91.62 \pm 1.56	91.59 \pm 2.42	96.12 \pm 0.93	92.23 \pm 1.52
	Uptake ratio of tumor/normal tissue				
Tumor/blood	1.18	6.27	8.00	2.40	1.00
Tumor/liver	1.44	2.31	2.38	1.89	0.49
Tumor/kidney	0.40	0.71	0.95	1.13	0.17
Tumor/lung	1.30	5.02	5.42	4.71	0.84
Tumor/muscle	10.61	65.20	30.55	11.00	7.33
Tumor/skin	1.01	5.53	4.94	2.81	1.20

* P<0.05 for determining significance of differences in tumor and kidney uptake between $^{99m}\text{Tc}(\text{EDDA})\text{-HYNIC-AocNle-CycMSH}_{\text{Hex}}$ with or without peptide blockade at 2 h post-injection.